E-ISSN: 2321–9637
Volume 2, Issue 1, January 2014
International Journal of Research in Advent Technology
Available Online at: http://www.ijrat.org

SYNTHESIS AND CHARACTERIZATION OF THIN FILMS OF PURE TIO_2 AND SR-DOPED TIO_2 PREPARED BY SPIN COATING TECHNIQUE

Mehul. H. Mngrola[1*] and Vibhuti. G. Joshi[1]
[1*]*Department of Sci. & Hum., Faculty of Engineering Technology & Research, Isroli-Bardoli, India.*
[1]*Department of Physics, Veer Narmad South Gujarat University, Surat-395006, India*
mhmangrola@gmail.com

ABSTRACT:
Transparent thin films of pure TiO_2 and 3% Sr-doped TiO_2 ($Ti_{0.97}$ $Sr_{0.03}O_2$) were prepared by spin coating technique onto well-cleaned glass substrate. These films were annealed at different temperatures. The structural analysis by GIXRD and Raman Spectroscopy confirms the anatase phase of TiO_2. The study also shows dependence of structural parameters and crystallinity on the annealing temperature of films. Surface morphology of the prepared films studied using Atomic Force Microscopy (AFM) exhibits a homogeneous globular structure. The UV-Visible analysis shows decrease in the optical band gap of the films annealed at higher temperatures. The UV spectra also show good absorbance of UV radiation in the wavelength range of 300 nm to 400 nm. Photoluminescence (PL) study shows variation in the emission peaks for films annealed at different temperature and for those with different concentrations of strontium (Sr). The dielectric properties, gas sensitivity, wettability and self-cleaning property of the prepared films were also studied and the results are discussed in details.

Key Words: *TiO_2 Film, GIXDR, RAMAN, AFM, UV, PL, Electrical property, CO_2 gas sensitivity, Wettability, Self-cleaning.*

1. INTRODUCTION

TiO_2 possesses three polymorphs: anatase, rutile and brookite, with distinct crystalline structures. The rutile is the most common and well known structure of the three. In rutile, the structure is based on octahedrons of TiO_2, which share two edges of the octahedron with other octahedrons and from chains Titanium dioxide (TiO_2) has attracted the attention of many research workers due to its outstanding physical and chemical properties. It is found that TiO_2 is also antibacterial, self cleaning and super hydrophilic. It has large number of applications as a catalyst support, gas sensor, thermoelectric and photovoltaic cells [1-13]. TiO_2 is also a promising material for next generation of ultra-thin capacitors, due to its dielectric property [14-15].

In the present work strontium (Sr) has been used as dopant. Alternating current conductivity (AC) measurements are used to characterize electrical properties of various materials and in the present work, it has been used for understanding the nature of conduction mechanism. Report are available for mesoporous STO film [16].

With increase in the frequency, the dielectric constant of the film is found to be decrease. This is because the frequency increases dipoles start to lag behind the field and dielectric properties is going to decrease and at higher frequency dipoles are not able to follow the field for longer. The AC conductivity is linearly increase with respect to frequency and Sr-doped TiO_2 show the low dielectric property and high AC conductivity compare with pure TiO_2 films [17].

Here we report on the structural, optical, electrical, gas sensitivity, wettability and self-cleaning properties of TiO_2 and Sr-doped TiO_2 thin films deposited by spin coating technique on glass substrate and post annealed at different temperature.

E-ISSN: 2321–9637
Volume 2, Issue 1, January 2014
International Journal of Research in Advent Technology
Available Online at: http://www.ijrat.org

2. EXPERIMENTAL & CHRACTERIZATION DETAILS

In the present work, six films (three for pure TiO_2 & three for Sr-doped TiO_2) of approximately 70-80 nm thickness were prepared. Titanium (IV) oxyacetylacetonate (0.3M) was used for Ti source and Strontium Chloride (GR) for Sr. Precursor samples were taken in polyethylene glycol (6ml) and water (4 ml). the solution was stirred for one hour at room temperature to obtain a viscous and transparent solution. The rpm of the spin coater was set at 2000 and during each rotation, three drops of solution were made to drop on the glass substrate. This process was repeated three times with the films being annealed at 300^0C between each process. One film each of TiO_2 and Sr-doped TiO_2 were then annealed for 30 minutes at 500^0C and 600^0C, respectively.

The films structure was studied by Grazing Incidence X-ray Diffraction (GIXRD) using Bruker D8 discover diffractometer, (Cu k_α radiation, λ=1.5406 Å) complementary information concerning film microstructure was derived from Raman Spectra which were acquired by means of a Jobin Yvon Horibra Labram- HR visible spectrometer using the blue line (488 nm) of an Ar laser as excitation source. The collection time for each spectrum was 5 minutes iin the range of 100 to 200 cm^{-1}.Film surface morphology were evaluated from AFM measurments. The photoluminescence emission spectra was obtained using Hariba Jobin Yvon Fluoro Ma-4 spectrofluorometer. UV absorption spectra was studied using Thermo Scientific evolution 600 UV-Visible Spectroscopy. The optical band gap for the films was calculated from “Tauc” equation plot. The dielectric loss and capacitance was measured as a function of frequency (100 Hz – 10 kHz) at room temperature in an air atmosphere using Hioki LCR meter. The gas sensitivity of the films in the presence of CO_2 gas has been measured using two probe method. In addition, the wettability and self-cleaning properties has also been investigated.

3. RESULT AND DISCUSSION

3.1 Structural Characterization

3.1.1 GIXRD Analysis

Figure 1(a) and 1(b), shows the GIXRD patterns of as deposited and annealed thin films of TiO_2 and Sr-doped TiO_2 film prepared by spin coating method on glass substrate. It is evident from GIXRD patterns that the annealed thin films are polycrystalline and shows anatase phase with preferential growth along (101) plane. The GIXRD pattern indicated the presence of (103), (200) and (101) planes of TiO_2 material which is in good agreement with JCPDS card no. 21-1272. The GIXRD pattern of as-deposited films low crystallinity. Intensity of (101) and (200) peaks increases as an effect of annealing, which is attributed to increasing crystallinity.

Separate peaks for Sr-doped TiO_2 are not observed due to low dopant concentration. It is also difficult to predict whether the Sr ion exists as Sr-O on the surface of TiO_2 as $SrTiO_3$ from the GIXRD pattern due to low dopant concentration.

E-ISSN: 2321–9637
Volume 2, Issue 1, January 2014
International Journal of Research in Advent Technology
Available Online at: http://www.ijrat.org

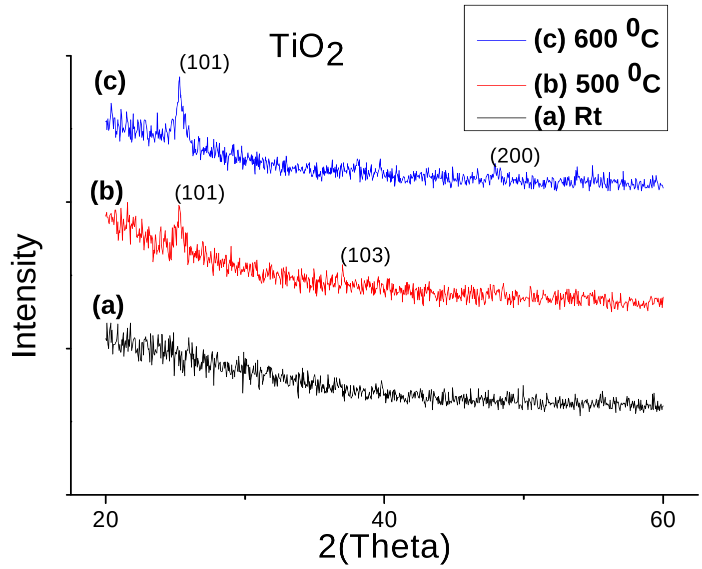

Fig. 1(a), GIXRD data of the TiO_2 thin films prepared by spin coating.

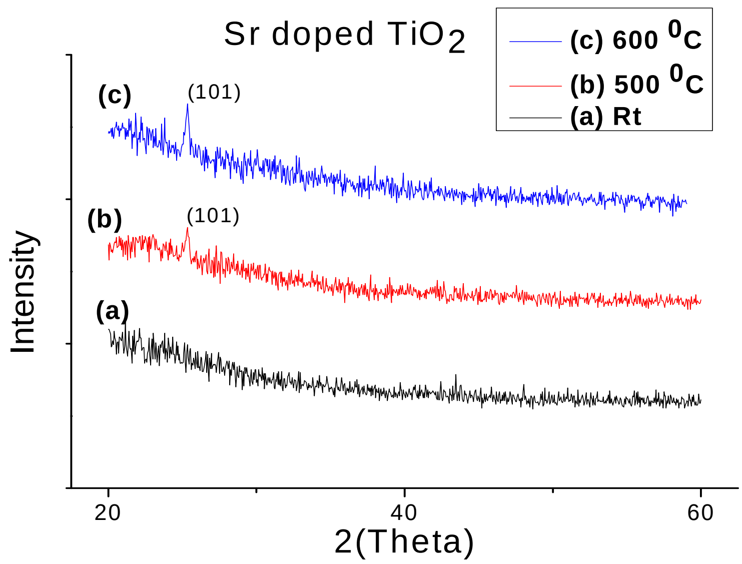

Fig. 1(b), GIXRD data of the Sr-doped TiO_2 thin films prepared by spin coating.

From the figure 1(a) and 1(b) it is clear that, without annealed film shows the amorphous nature and as we increase the annealing temperature the crystallinity of the film also increase. The anatase phase of TiO_2 was found in both samples annealed at high temperature. The crystalline size estimate using the Debye-Scherer formula is found to be 32 nm for pure TiO_2 and 37 nm for Sr-doped TiO_2.

We have used short and long time scan because of very low thickness of film and we took scan in the range of 100 to 200 cm^{-1}. The main peak of anatase phase of TiO_2 is observed near about 144 cm^{-1}. The Raman spectroscopy of the samples confirms the anatase phase of TiO_2 as determined by GIXRD analysis.

3.2 Raman Spectroscopy Analysis

E-ISSN: 2321–9637
Volume 2, Issue 1, January 2014
International Journal of Research in Advent Technology
Available Online at: http://www.ijrat.org

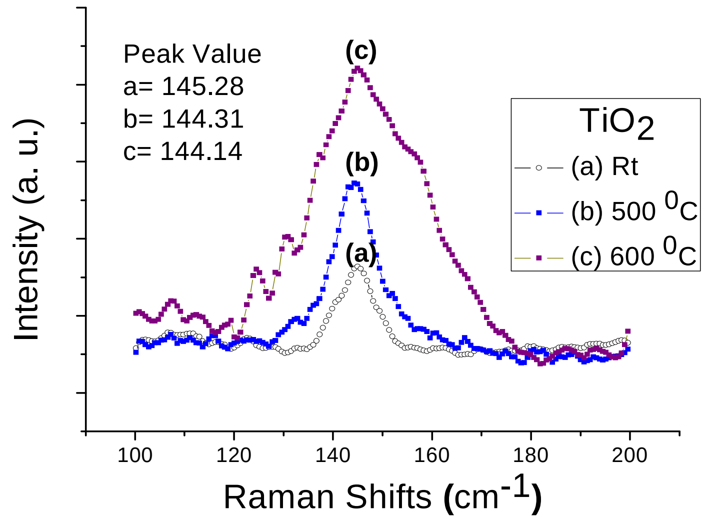

Fig. 2(a), Raman spectra of TiO_2 thin film prepared by spin coating technique.

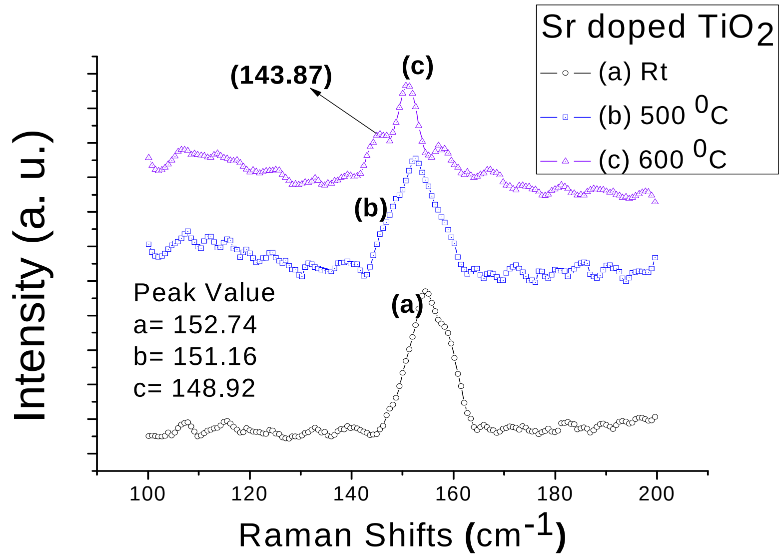

Fig. 2(b), Raman spectra of Sr-doped TiO_2 thin film prepared by spin coating technique.

Raman spectra shows broadening of the spectra with increase in annealing temperature. Post annealed film also show the shifting. Same result were observed in Sr-doped TiO_2 films but in whole sample we get peak near about 149 cm^{-1} [18-20] and they are also shows the same type of shifting compare with TiO_2 Raman spectra. This result supports that the structural parameter is dependent on the annealing temperature and anatase phase is more temperature sensitive and TiO_2 shows the anatase to rutile phase transformation at high temperature. The Raman shifting of Sr-doped TiO_2 spectra also indicates that Sr is properly combined/attached with Ti atom.

3.3 AFM Analysis

E-ISSN: 2321–9637
Volume 2, Issue 1, January 2014
International Journal of Research in Advent Technology
Available Online at: http://www.ijrat.org

The formation of TiO_2 and thin films deposited by spin coating is considered accumulating like “tiny island”. Figure 3 shows the surface topography image of sample obtained by AFM. All the as-deposited thin films indicates surfaces which are not highly rough, and that the film is homogeneously distributed on the substrate. Without post annealed films show rough surface compare to annealed films. The 2D image of the films show the spherical shape of the particles and post annealed films also show same result but compare to without annealed film the particle size is small and of uniform spherical shape. The particle size calculated from the AFM data is near about ~115 nm in post annealed films in both samples. From the AFM result, it is believed that the thin film grow process consist of three aspects, the atoms adsorption, migration and desorption, which are all connected with the annealed temperature and viscosity of the sample solutions. AFM Images obtained on different regions of the samples showed that the films exhibit a homogeneous globular structure. The entire film surface is formed by small grains of the deposited material.

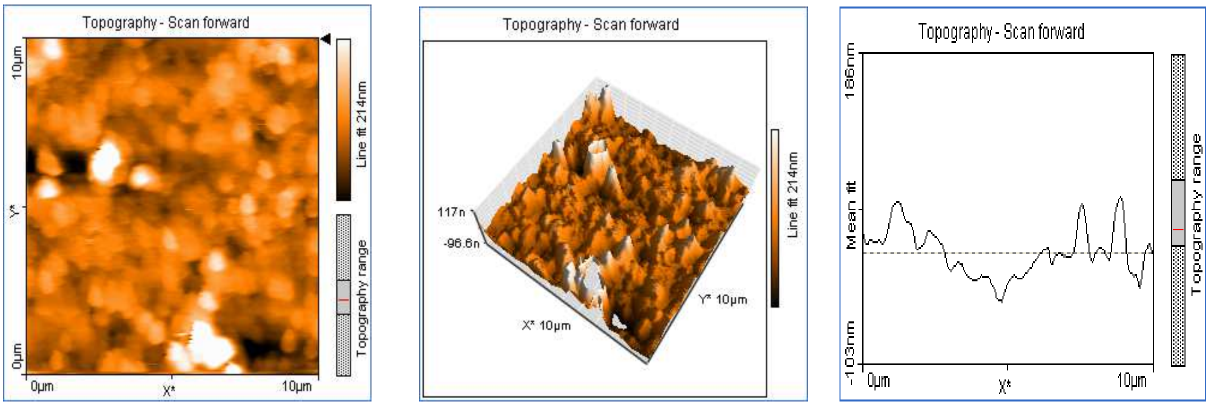

Fig. 3(a), AFM data of TiO_2 thin film annealed at 600^0C

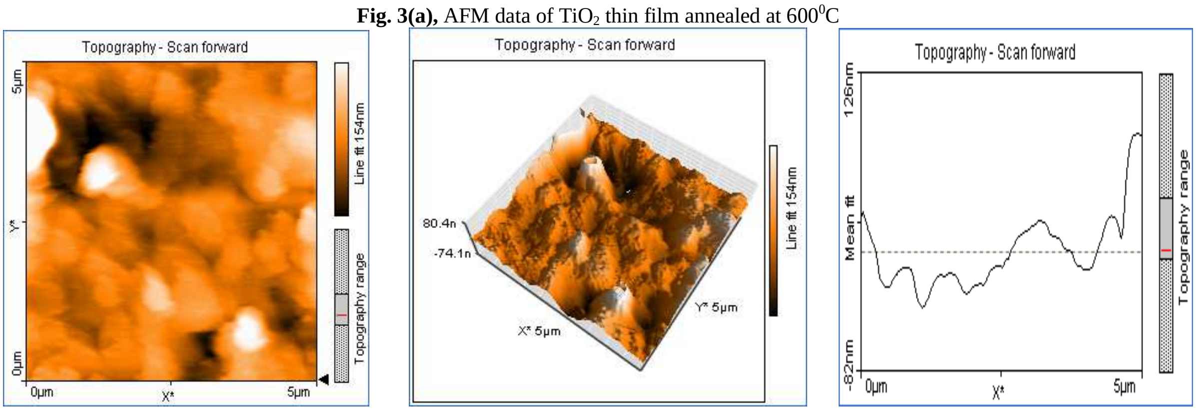

Fig. 3(b), AFM data of TiO_2 thin film annealed at 500^0C

E-ISSN: 2321–9637
Volume 2, Issue 1, January 2014
International Journal of Research in Advent Technology
Available Online at: http://www.ijrat.org

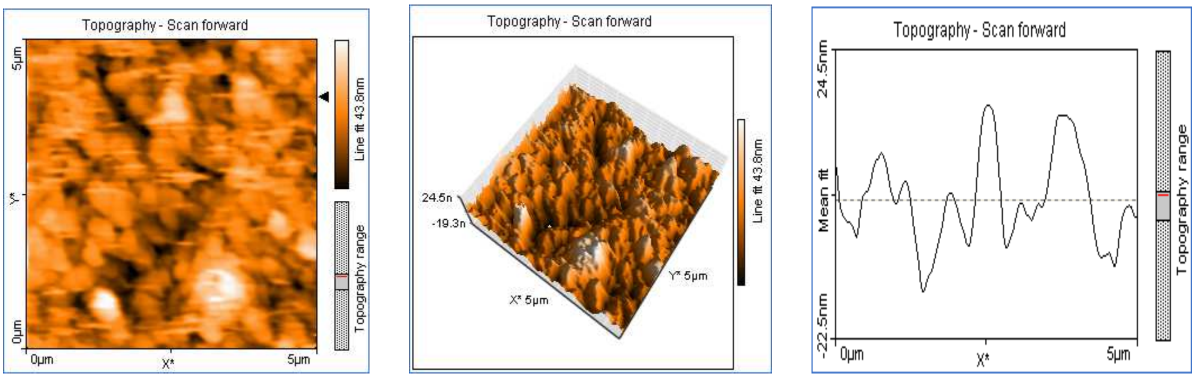

Fig. 3(c), AFM data of Sr doped TiO_2 thin film annealed at 600^0C

3.4 UV-Visible Spectroscopy Analysis

Figure 4a and 4d shows the UV-Visible spectra of pure TiO_2 and Sr-doped TiO_2 and figure 4b and 4c show the Tauc plot of pure TiO_2 and Sr-doped TiO_2 thin films.

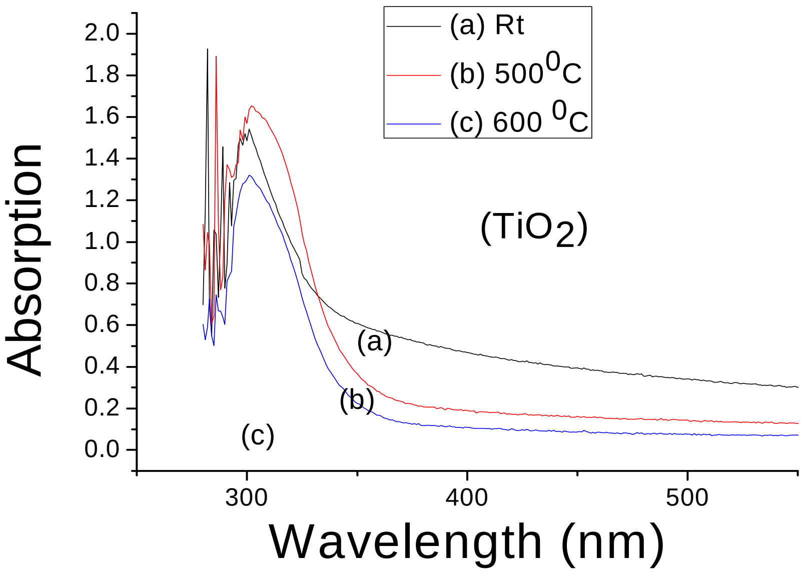

Fig. 4a, UV-spectra of TiO_2 films

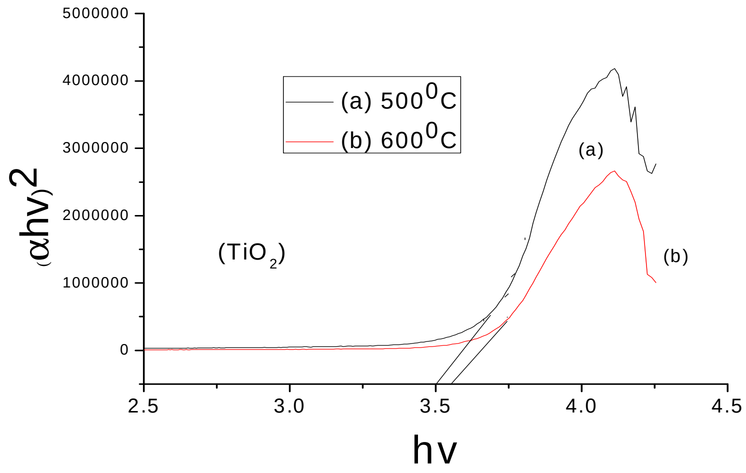

Fig. 4b, Tauc plot of TiO_2 films

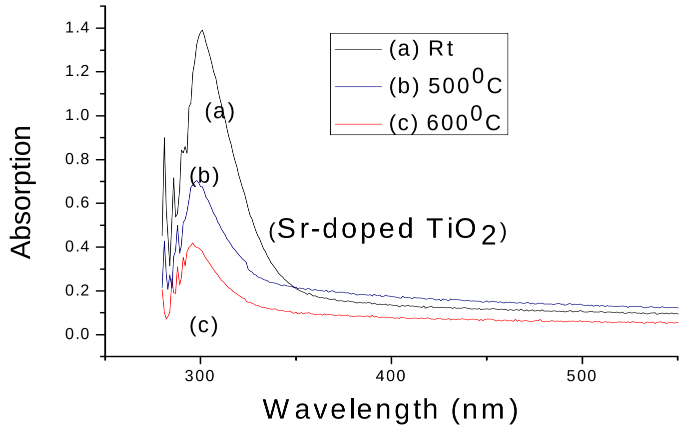

Fig. 4c,UV-spectra of Sr-doped TiO_2 films

E-ISSN: 2321–9637
Volume 2, Issue 1, January 2014
International Journal of Research in Advent Technology
Available Online at: http://www.ijrat.org

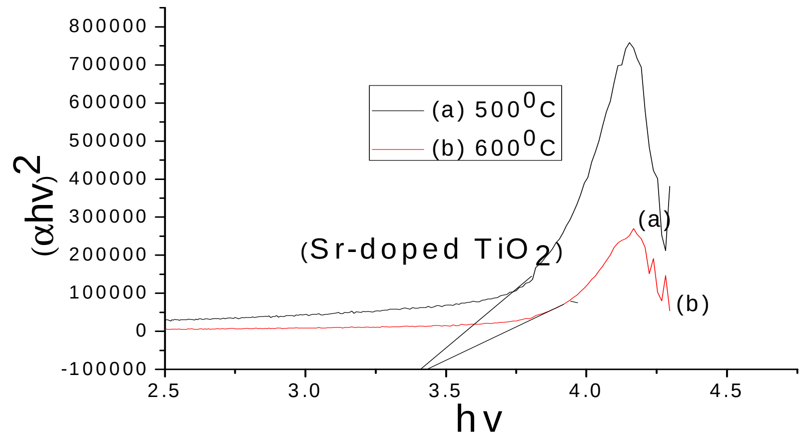

Fig. 4d,Tauc plot of Sr-doped TiO_2 films

From the figure 5, it is clearly observed that the absorption varies with the annealing temperature of the Sr-doped TiO_2 films. This indicates that the optical property of the TiO_2 thin films depends on the annealing temperature. When we annealed the film the oxidation of the film changes the optical property, surface property and density of the TiO_2 film. UV-Visible absorption spectral analysis is used to probe the band structure of materials. The absorbance edges changes with annealing temperature. Some work has been reported on the optical property of the TiO_2 with doping of foreign element [21-22].

UV analysis shows that the optical band gap of the films, estimated using the Tauc plot increases from 3.5 to 3.6 eV for pure TiO_2 thin film on increasing the annealing temperature. It is also seen that for 3% Sr-doped TiO_2 thin film, the band gap increases from 3.4 to 3.45 eV. It is found that the films after post annealing show good optical transmittance near the UV-Visible region. This shows that strontium influences on the optical behaviour of TiO_2 and that Sr-doped TiO_2 film can be used as UV sensor.

3.5 Photoluminescence Analysis

Figure 5, shows the photoluminescence emission spectra for the prepared films. The emission spectra were measured at different excitation wavelength in the range of 280 nm to 550 nm. In this work, the emission spectra were not observed at the 280 nm and above 500 nm excitation wavelength. The emission spectra were observed in the range between 300 to 500 nm. The PL behaviour of the Sr-doped TiO_2 also shows similar behaviour.

E-ISSN: 2321–9637
Volume 2, Issue 1, January 2014
International Journal of Research in Advent Technology
Available Online at: http://www.ijrat.org

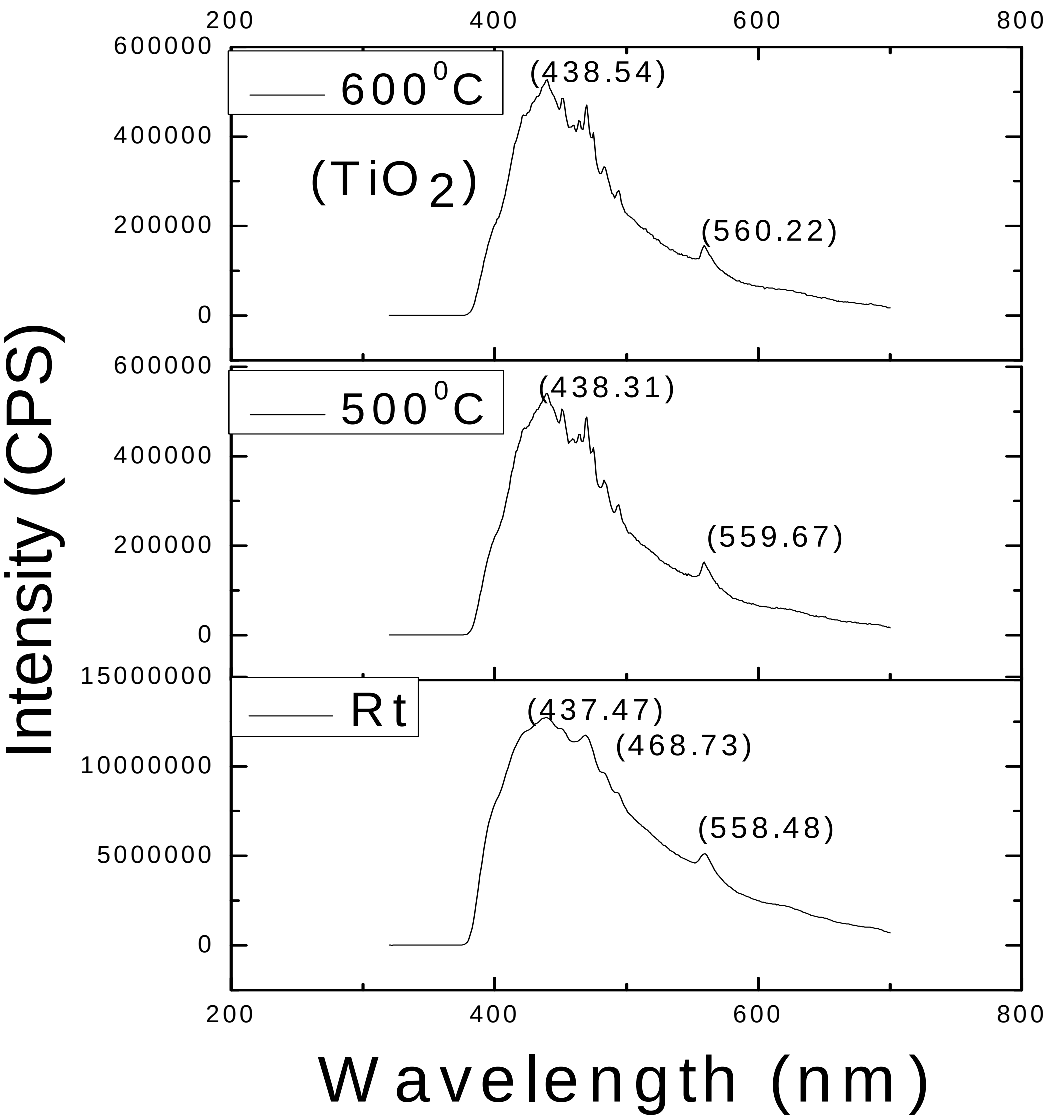

Fig. 5a, PL emission spectra of TiO_2 films (Ex. Wavelength = 300 nm)

E-ISSN: 2321–9637
Volume 2, Issue 1, January 2014
International Journal of Research in Advent Technology
Available Online at: http://www.ijrat.org

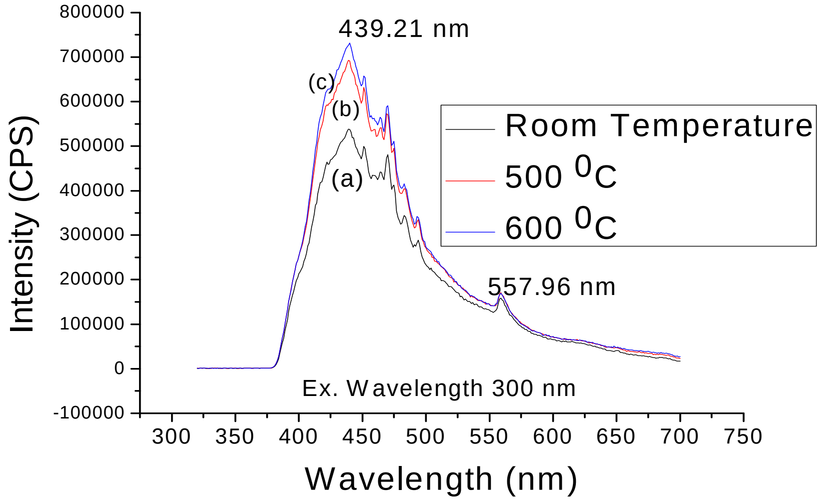

Fig. 5b, PL spectra of Sr-doped TiO_2 films

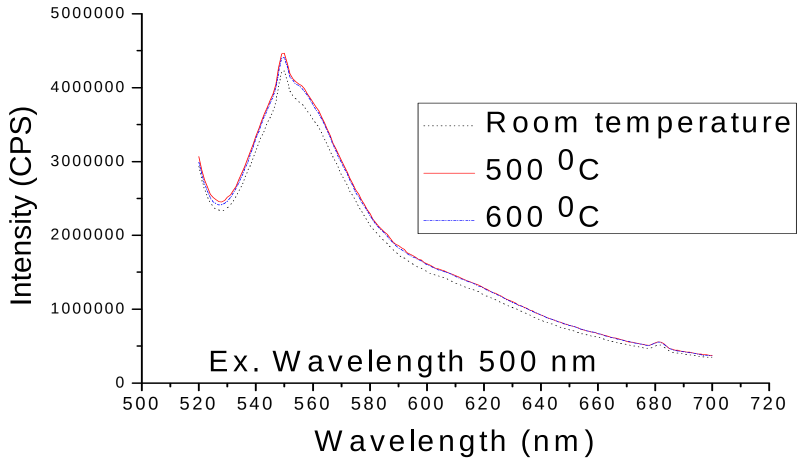

Fig. 5c, PL spectra of Sr-doped TiO_2 film

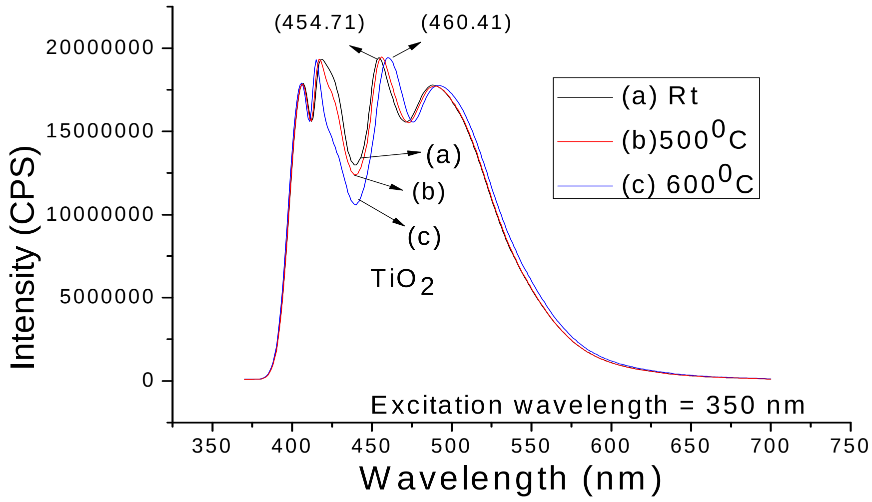

Fig. 5d, PL spectra of TiO_2 films

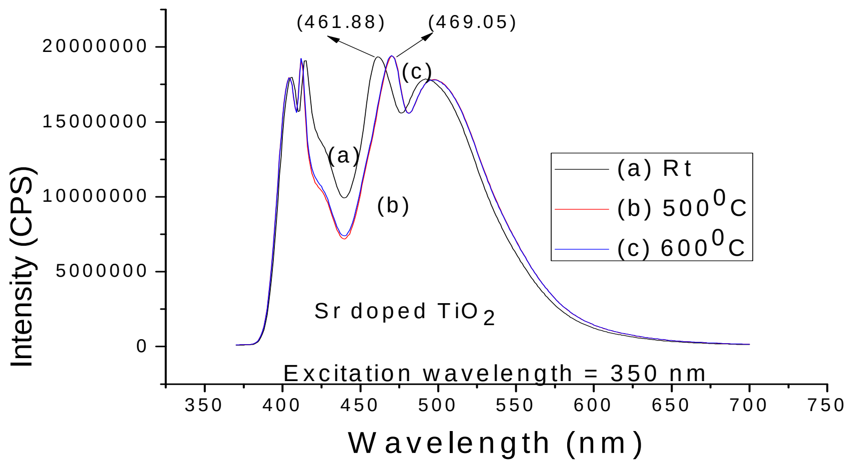

Fig. 5e, PL spectra of Sr-doped TiO_2 films

Figure 5a and 5b shows the PL emission spectra of TiO_2 and Sr-doped TiO_2 for the excitation wavelength of 300 nm respectively and figure 5c shows the emission spectra of Sr-doped TiO_2 at the excitation wavelength of 500 nm. Figure 5d and 5e shows the PL emission spectra of pure TiO_2 and Sr-doped TiO_2 at the excitation wavelength of 350 nm. For both these excitation wavelengths the PL emission spectrum is observed in the visible range. The PL behaviour of the anatase TiO_2 is also depending on the grain size [23]. The visible PL emission of the anatase TiO_2 is due to lattice defects of vacancies and charge interstitial.

In present work, all films prepared are highly transparent. At the 300 nm excitation wavelength, sharp peak were observed for both films, and the annealing temperature is increase with respect to the maximum peak value which shows a shift to higher wavelength in both films. The shifting difference in without annealed and post-annealed films is 1 to 3 nm. At the excitation wavelength of 350 nm, same behaviour is observed but at this excitation wavelength 3-4 emission peak is observed.

E-ISSN: 2321–9637
Volume 2, Issue 1, January 2014
International Journal of Research in Advent Technology
Available Online at: http://www.ijrat.org

In both excitation wavelengths, the visible emission is observed in the range of 380 nm to 550 nm. The visible emission of anatase TiO_2 and actual mechanism behind the visible emission of anatase TiO_2 film and bulk is due to radiative emission of self-trapped excitation theory of Toyozawa [24-26]. The present study, shows the annealing temperature greatly influences the PL behaviour of TiO_2 and doping concentration is highly effective in adjusting the Fermi energy level for semiconductor [27].

3.6 CO_2 Gas Sensitivity

Figure 6, shows the graph of sensitivity versus operating temperature for the post annealed films. The setup for measuring the gas sensitivity behaviour of the samples was developed in laboratory. In order to understand the temperature dependence sensitivity of TiO_2 thin film specimen CO_2 gas with concentration of about 100 ppm was used. An external voltage of 5 volt was used during measurements. In our measurement we observed that as the temperature of the sample is increased the gas sensitivity also increases and they reach a maximum value for 255^0C temperature. At higher temperature it decreases. The annealing temperature and doping concentration also affects the gas sensitivity of the TiO_2. A Sr-doped TiO_2 film shows high sensitivity, as compared to pure TiO_2. The sensitivity of the semiconductor gas sensor is mainly determined by the interaction between the target gas and the surface of the sensors. The greater the surface area of the materials stronger is the interaction between the absorbed gases and sensor surface.

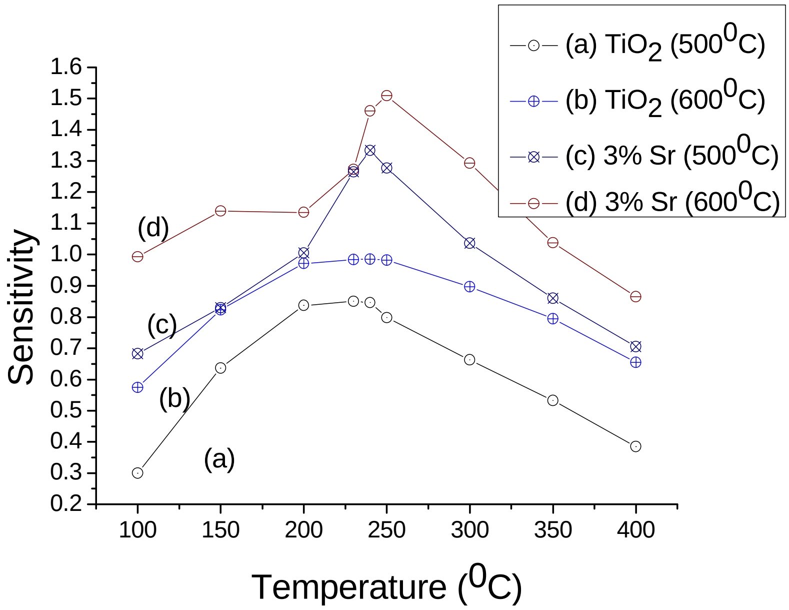

Fig. 6, sensitivity versus operating temperature of the films

Figure 7, shows the sensitivity as a function of operating time for films annealed at a temperature of 255 ± 5^0C. A rapid increase in sensitivity with increasing time is observed. This is because, greater surface area of the materials provides stronger interaction between the adsorbed gases and the sensor surface. i.e. higher gas sensitivity of the film because the surface species and trapped electron are return to the conduction band causing an increase in the conductivity of the films. Sr-doped TiO_2 shows the high gas sensitivity compare with pure TiO_2.

In general, the high temperature operation of the sensor makes the life time of the sensor shorter and increases resistance thus consuming more power for operation. It is believed that the oxygen could be removed or is lost from the materials/film surface at high temperature. This suggests that the response of the sensor may decrease at high temperature. Since there will be more oxygen vacancies which led to less occurrence of CO_2 oxygen reaction. Also the sensing process depends on the surface roughness of the TiO_2 films.

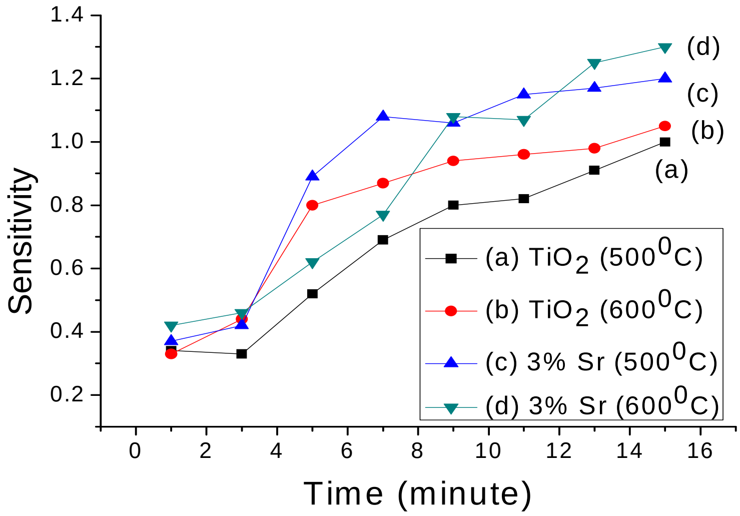

Fig. 7, Sensitivity versus time at 255^0C

Figure 8, shows the graph of resistance as a function of time of operation at 255^0C temperature for the films. Pure TiO_2 film shows the high resistance compare with Sr-doped TiO_2 films. Resistance gradually decreases due to the increasing in the sensing current of the film.

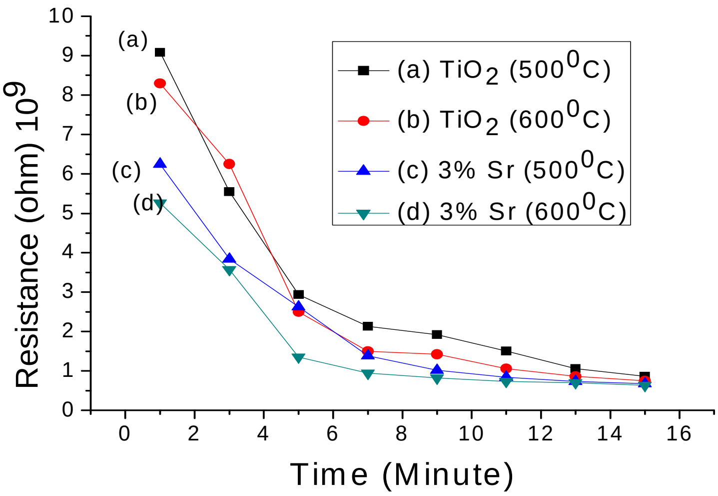

Fig. 8, Resistance as a function of time at 255^0C

Figure 9, shows the graph of current as a function of time. Without doping and without annealed film shows low current as compare to doped and post-annealed film. At 600^0C annealed Sr-doped TiO_2 film shows high current at about 8 nA.

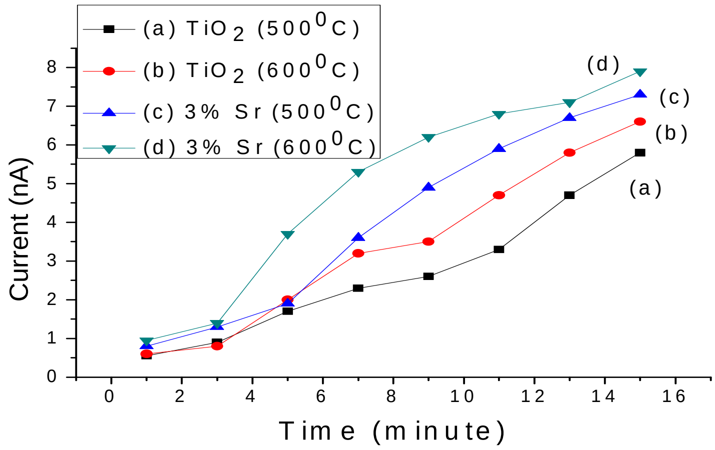

Fig. 9, Current versus time at 255^{0}C

The current value of pure TiO_2 film is very less compare with Sr-doped TiO_2 film, is due to the surface species and trapped electrons are returned to the conduction band causing an increase in the conductivity of the TiO_2 film doping with strontium and respectively the current value of sensor increase.

3.7 Self-Cleaning Properties

Figure 10a & 10b shows the self-cleaning activity of the films. Figure 10a, (A, B, C) shows the self-cleaning activity at the Room temperature of the TiO_2 film annealed at 500 ^{0}C and annealed at 600 ^{0}C and D, E, F for Sr-doped TiO_2 film. Figure 10b, all same but after two days exposed in sun light. TiO_2 shows the photo catalytic activity and because of that it has ability to decompose the organic dirt molecules in the presence of UV light or sun light. In present study, it is observed that when the droplets of red ink (fountain pen ink, Camel production) dye was put on the both coated and uncoated glass substrate. It is observed that, the post annealed film shows high self-cleaning activity as compare to that without annealed. The Sr-doped TiO_2 films shows more cleaning activity after two days as compared with pure TiO_2 coated films.

Post-annealed film shows high self-cleaning activity of the films. This result also suggests that the self-cleaning activity depends on surface morphology and crystallinity of the film. In both case Sr-doped TiO_2 films shows more self-cleaning activity as compared with pure TiO_2 films.

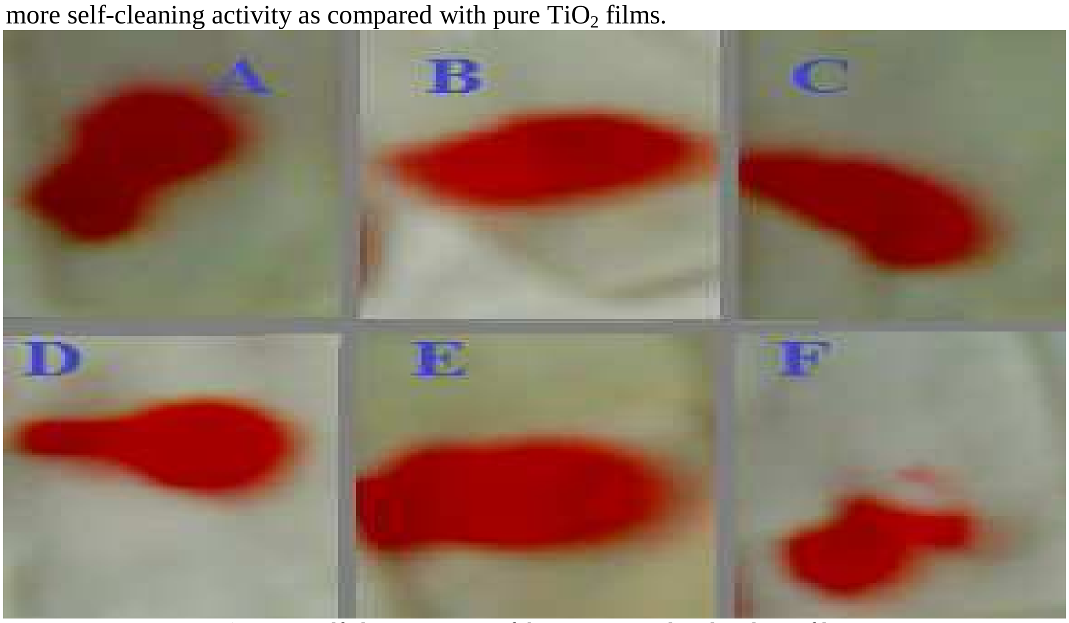

Fig. 10a, Self-cleaning activity of the pure TiO_2 and Sr-doped TiO_2 films

E-ISSN: 2321–9637
Volume 2, Issue 1, January 2014
International Journal of Research in Advent Technology
Available Online at: http://www.ijrat.org

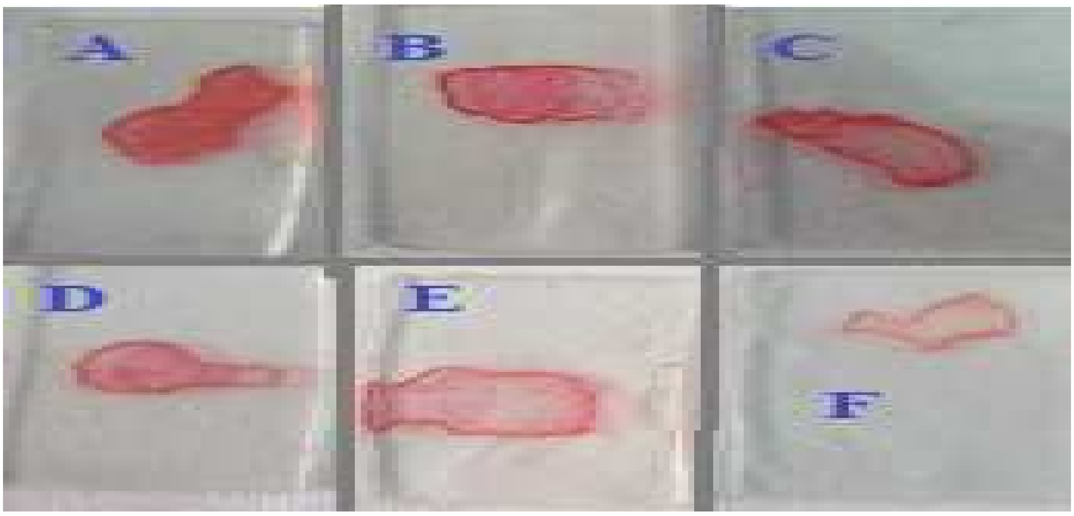

Fig. 10b, The self-cleaning activity of the pure TiO_2 and Sr-doped TiO_2 films (After exposure to in sun light for two days)

TiO_2 shows photo-catalytic property and because of that it has ability to decompose the organic dirt molecules in presence of UV light or sun light. In present work, it is observed that when the droplet of red (fountain pen red ink, camel) dye was put on both coated and uncoated glass, the coated glass was seen more clean as compared with uncoated glass substrate.

3.8 Wettability Analysis

In the present work, we studied the surface hydrophilicity of the TiO_2 and Sr-doped TiO_2 films. It was quantified from measurements of the water contact angle on the without coated and with coated glass substrate. The measurement was first performed on normal ordinary glass and there after for TiO_2 and Sr-doped TiO_2 coated glass substrate for the same time duration. It is observed that the contact angle of water droplet is very less compare with dopant TiO_2. Sr-doped TiO_2 shows the higher contact angle in without annealed and post annealed film compare with pure TiO_2. Post annealed film shows the large contact angle, which indicates that the crystallinity of the sample is also important for the hydrophobic and hydrophilic behaviour of TiO_2 and Sr-doped TiO_2 films. Figure 11 shows the wettability behaviour of the pure TiO_2 and Sr-doped TiO_2 films prepared by spin coating method [28-29].

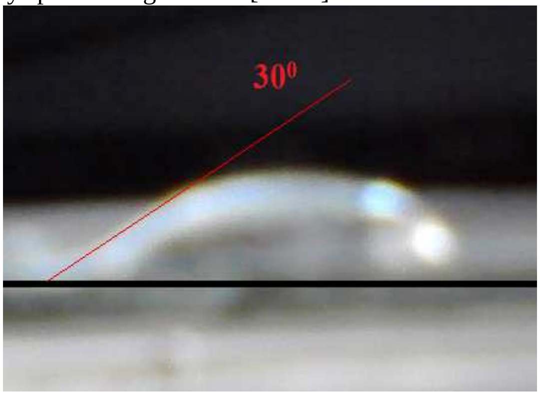

Fig. 11a, Pure TiO_2 coated film (without annealed)

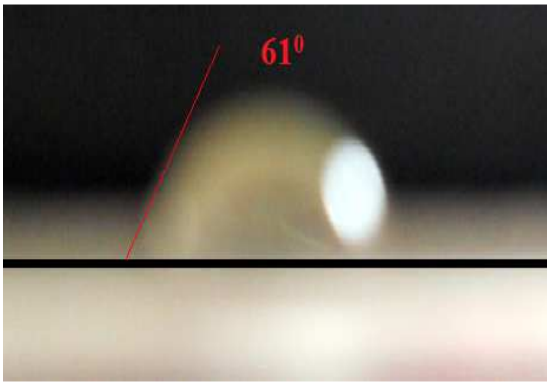

Fig. 11b, Pure TiO_2 coated film (annealed at 600^0C)

E-ISSN: 2321–9637
Volume 2, Issue 1, January 2014
International Journal of Research in Advent Technology
Available Online at: http://www.ijrat.org

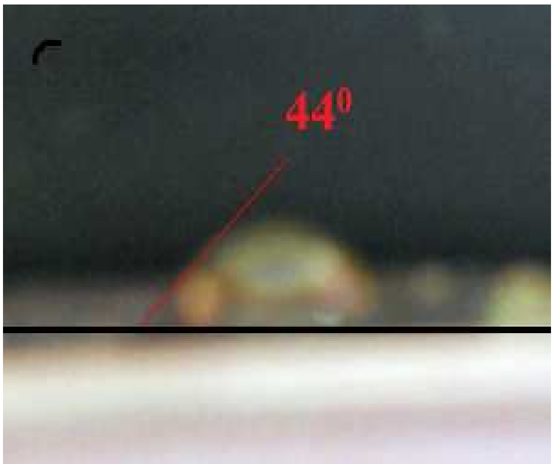

Fig. 11c, Sr-doped TiO_2 coated film (without annealed)

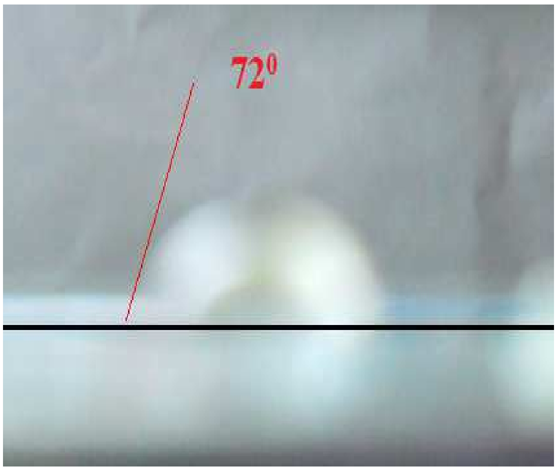

Fig. 11d, Sr-doped TiO_2 coated film (annealed at 600^0C)

4. CONCLUSION

Thin films shows the amorphous nature at room temperature (without annealed film) and post annealed film shows that the crystallinity of the films increases for the anatase phase of TiO_2. Raman data suggests that the anatase phase is present in the prepared TiO_2 film. The Raman spectrum shows shifting with increase in doping concentration. Raman data strongly supports the GIXRD data. The strontium doped TiO_2 film also shows changes in band gap with doping concentration and calcination of film. Without annealed films shows less intense PL emission spectra with sharp peak and the intensity of the peaks are found to increase with annealing temperature. Doping does not seem to influence the intensity of the peak but peak positions are found to shift. Films shows CO_2 gas sensitivity of 0.8. The sensitivity of the both films is found to increase with the function of time and resistance decreases with function of time. Strontium doped TiO_2 films shows increment in the CO_2 gas sensitivity of the films and also shows increases in sensitivity with operation function of time whereas resistance decreases with function of time. Spin coating shows high self-cleaning activity observed in post annealed film and low self-cleaning activity observed in without annealed film. Post-annealed strontium doped TiO_2 films shows the very high self-cleaning activity as compared with without annealed film. Strontium doped TiO_2 films also shows high contact angle with water.

Acknowledgement

Rajiv Gandhi UGC fellowship to one of the authors (M. H. Mangrola) is fully acknowledged. The authors also wish to thank UGC DAE CSR Indore, Dr. B. S. Chakrabarty (Applied Physics Department, M. S. University of Baroda), Dr. Vandana N Rao (Metallurgy & Material Science Department, M. S. University of Baroda), Dr. Utpal Joshi (School of Science, Department of Physics, Gujarat University) and Dr. M. Roy (M. L. Sukhadiya University, Udaipur) for their support and valuable suggestions.

References

[1] Nakaruk and Lin C., Perera D. and Sorrell C., (2010) J Sol-Gel Sci Technol , 55, 328.
[2] Hemissi M. and Amardjia-Adnani H., (2007) Digest J. of Nanomaterials and Biostructures, 2, 299.
[3] Kaczmarek D., Wojcieszak D., (2011) et. al., Cent. Eur. J. Phys., 9 (2), 349.
[4] Stamate M., Vascan I., Lazar I., Caraman I. and Caraman M., (2005) J. of Optoelectronics and Adv. Mate., 2, 771.
[5] Catherine Blount M., Hyun Kim D. and John L. Falconer, (2001) Environ. Sci. Technol. 35, 2988.
[6] Caricato A., Buonsanti R., (2011) et. al. Appl. Phys. A., 104, 963.
[7] Akbar S., Dutta P. and Lee C., (2006) Int. J. Appl. Ceram. Technol., 3(4), 302.
[8] Mene R., Mahabole M., Aiyer R. and Khairnar R., (2010) The Open Applied Physics Journal, 3, 10.
[9] Telipan G., Ignat M., Tablet C. and Parvulescu V., (2008) J. of Optoelectronics and Materials, Vol. 10, No. 8, 2138.

[10] Dubal D., Dhawale D. , More A. and Lokhande C., (2011) J Mater Sci, 46, 2288.
[11] Shengyuan Y., Peining Z., Sreekumaran Nair A. and Ramakrishna S., (2011) J. Mater. Chem. 21, 6541.
[12] Kumaresan L., Mahalakshmi M., Palanichamy M. and Murugesan V., (2010) Ind. Eng. Chem. Res. 49, 1480.
[13] Cui C., He J., Amow G. and Kleinke H., (2010) Dalton Trans., 39 1031.
[14] Te-Cheng Mo, Hong-Wen Wang, San-Yan Chen and Yun-Chieh Yeh, (2008) Ceramics International 34, 1767.
[15] Valentin Bessergenev, (2009) Materials Research Bulletin 44, 1722.
[16] Mohammadi M. and Fray D., (2011) J. Coat. Technol. Res., 8(5), 585.
[17] Mangrola M., Pillai A., Parmar B., Joshi V., (2013) Advanced Materials Research Vol. 665, 263.
[18] Niilisk A., Moppel M., (2006) et. al., Cent. Eur. J. Phys. 4(1), 105.
[19] Nilsen W. and Skinner J., (1968) The J. of Chemical Physics, 48 (5), 2240.
[20] Bersani D., Antonioli G., Lottici P., Lopez T., (1998) Journal of Non-Crystalline Solids 232±234, 175.
[21] Karki, Gnanasekar K. and Rambabu B., (2006) Appl. Sur. Sci., 193-195, 399.
[22] Thi Thanh Lea D., Vuongb D., and Van Duya N., (2009) Proceedings of the Eighth German -Vietnamese Seminar on Physics and Engineering, Erlangen.
[23] Zhang W., Zhang M., Yin Y., Chen Q., (2007) Appl. Phys. B 70, 261.
[24] Tang H., Berger H., Schmid P. and Levy F., (1993) Solid State Communication, Vol. 87, No.9, 847.
[25] Toyozawa Y., (1976) J. Luminescence., 12/13, 13.
[26] Toyozawa Y., (1980) in relaxation of elementary Excitation (Edited by R. Kubo & E. Hanamura), p. 3 Springer-Verlag, New York.
[27] Sze S., (1981) Physics of semiconductor devices, p. 84.
[28] Janczarek M., Hupka J. and Kisch H., (2006) Physicochemical Problem of Mineral Processing, 40, 287.
[29] Kwang-Dae Kim, Wei Sheng Tai, et. al., (2009)Bull. Korean Chem. Soc., Vol. 30, No. 5, 1067.